Nectin-like proteins mediate axon–Schwann cell interactions along the internode and are essential for myelination

Patrice Maurel,[1] Steven Einheber,[2] Jolanta Galinska,[1] Pratik Thaker,[1] Isabel Lam,[1] Marina B. Rubin,[1] Steven S. Scherer,[3] Yoshinuri Murakami,[4] David H. Gutmann,[5] and James L. Salzer[1]

[1]Department of Cell Biology and Neurology, Smilow Neuroscience Program, New York University School of Medicine, New York, NY 10016
[2]City University of New York, Hunter College, New York, NY 10010
[3]Department of Neurology, University of Pennsylvania School of Medicine, Philadelphia, PA 19104
[4]Department of Cancer Biology, Institute of Medical Science, The University of Tokyo, Tokyo 108-8639, Japan
[5]Department of Neurology, Washington University School of Medicine, St. Louis, MO 63110

Axon–glial interactions are critical for the induction of myelination and the domain organization of myelinated fibers. Although molecular complexes that mediate these interactions in the nodal region are known, their counterparts along the internode are poorly defined. We report that neurons and Schwann cells express distinct sets of nectin-like (Necl) proteins: axons highly express Necl-1 and -2, whereas Schwann cells express Necl-4 and lower amounts of Necl-2. These proteins are strikingly localized to the internode, where Necl-1 and -2 on the axon are directly apposed by Necl-4 on the Schwann cell; all three proteins are also enriched at Schmidt-Lanterman incisures. Binding experiments demonstrate that the Necl proteins preferentially mediate heterophilic rather than homophilic interactions. In particular, Necl-1 on axons binds specifically to Necl-4 on Schwann cells. Knockdown of Necl-4 by short hairpin RNA inhibits Schwann cell differentiation and subsequent myelination in cocultures. These results demonstrate a key role for Necl-4 in initiating peripheral nervous system myelination and implicate the Necl proteins as mediators of axo–glial interactions along the internode.

Introduction

Myelinated axons are organized into a series of discrete domains that are distinguishable by their molecular composition and physiological function. These domains include the nodes of Ranvier, which are enriched in voltage-gated sodium channels essential for saltatory conduction, the flanking paranodal junctions, and the juxtaparanodes, which are enriched in Shaker type K^+ channels (Poliak and Peles, 2003; Salzer, 2003). Each of these domains forms as the result of instructive contact-dependent signals from myelinating glia (i.e., Schwann cells in the peripheral nervous system [PNS] and oligodendrocytes in the central nervous system). Adhesion molecules on the glial cell bind to and recruit a complex of axonal adhesion molecules and cytoskeletal proteins; the latter include ankyrin G at the node and 4.1B at the paranodes and juxtaparanodes. Interactions with these cytoskeletal proteins target and stabilize the localization of additional proteins (i.e., sodium channels at the node and potassium channels at the juxtaparanodes). However, together, these domains (the node, paranodes, and juxtaparanodes) only account for ~1% of the longitudinal extent of the axon.

The remaining and by far the largest domain of the myelinated axon is the internode, the portion of the axon located under the compact myelin sheath. Axons and myelinating glia exhibit an intimate functional relationship in this region, as reflected in the highly regular apposition of their respective plasma membranes, which are separated by 12–13 nm. This separation persists after osmotic changes or in various pathologic states (Hirano, 1983). Conversely, the periaxonal space as well as attachment of the myelin sheath to the axon is disrupted by the action of proteases (Yu and Bunge, 1975). These results indicate that interactions between the glial and axonal membranes along the internode are actively maintained by cell surface proteins.

The molecules that mediate axonal–glial interactions along the internode have remained largely elusive. The myelin-associated

Correspondence to Patrice Maurel: maurep01@med.nyu.edu; or James L. Salzer: Salzer@Saturn.med.nyu.edu

Abbreviations used in this paper: dPBS, Dulbecco's PBS; DRG, dorsal root ganglion; FERM, 4.1, ezrin, radixin, moesin; MAG, myelin-associated glycoprotein; MBP, myelin basic protein; Necl, nectin-like; PDZ, PSD-95, DLG, Z01; PE, phycoerythrin; PNS, peripheral nervous system; shRNA, short hairpin RNA; SynCAM, synaptic cell adhesion molecule; TSLC1, tumor suppressor in lung cancer 1.

The online version of this article contains supplemental material.

The Journal of Cell Biology, Vol. 178, No. 5, August 27, 2007 861–874
http://www.jcb.org/cgi/doi/10.1083/jcb.200705132

glycoprotein (MAG), a member of the Ig superfamily expressed by myelinating Schwann cells and oligodendrocytes, has been specifically localized to this region (Trapp, 1990). MAG is expressed in the periaxonal glial membrane at initial stages of myelination (Martini and Schachner, 1986) and interacts with several axonal components (Hannila et al., 2007); at later stages of myelination, it localizes to Schmidt-Lanterman incisures as well (Trapp, 1990). However, mice deficient in MAG myelinate appropriately and exhibit only modest alterations in the periaxonal space (Li et al., 1994; Montag et al., 1994), suggesting that other molecules are likely to mediate axo–glial adhesion along the internode.

Recently, a family of adhesion molecules termed the Nectin-like (Necl) proteins were described (Sakisaka and Takai, 2004). Like the nectins, a family of adherens junction proteins, the Necl proteins contain three extracellular Ig-like domains, a single transmembrane domain, and a short cytoplasmic segment (Fig. 1 A). Necl proteins notably differ from the nectins in their cytoplasmic sequences, which are linked to the cytoskeleton via a FERM (4.1, ezrin, radixin, moesin)-binding domain in their juxtamembrane region and contain a class II PDZ (PSD-95, DLG, Z01)-binding sequence at their C terminus. The Necl proteins have been implicated in a variety of biological activities, including cell adhesion, regulation of cell growth and synaptic function, and cell polarity (for review see Ogita and Takai, 2006). They were originally identified as tumor suppressor in lung cancer 1 (TSLC1)–like proteins, as their limited expression in lung cancer cell lines (Gomyo et al., 1999; Fukuhara et al., 2001; Kuramochi et al., 2001) and other tumor types (Murakami, 2005) correlates with abnormal cell proliferation. They have also been shown to promote synapse formation and glutamate receptor clustering, leading to an alternative designation as synaptic cell adhesion molecules (SynCAMs; Biederer et al., 2002).

Five Necl proteins have been identified, each independently by several groups, which accounts for the diverse nomenclature. The Necl proteins include Necl-1/TSLL1/SynCAM3/IgSF4B (Fukuhara et al., 2001), Necl-2/TSLC1/SynCAM1/IGSF4/RA175/SgIGSF (Urase et al., 2001; Ito et al., 2003; Shingai et al., 2003), Necl-3/SynCAM2, Necl-4/TSLL2/SynCAM4, and Necl-5/Tage4 (Ikeda et al., 2004). As Necl-5 lacks the characteristic FERM- and PDZ-binding motifs of the cytoplasmic domain, its classification as a member of the Necl family is controversial (Dong et al., 2006). Necl-2 is the prototype and most intensively studied member of this family. It is widely and highly expressed, including in the developing nervous system and various epithelial tissues (Fukuhara et al., 2001; Urase et al., 2001; Fujita et al., 2005). Necl-2 promotes adhesion via homophilic (Biederer et al., 2002; Masuda et al., 2002; Shingai et al., 2003) and heterophilic interactions (Shingai et al., 2003). Like other Necl proteins (Dong et al., 2006; Williams et al., 2006), Necl-2 is believed to mediate adhesion as a cis-dimer. Necl-2 has been reported to interact intracellularly with DAL1, a truncated form of the band 4.1B protein (Yageta et al., 2002). Other Necl proteins are highly expressed in the nervous system, including Necl-1 (Fukuhara et al., 2001; Gruber-Olipitz et al., 2006) and Necl-4 (Dong et al., 2006). They are inferred to mediate adhesion although their ligands, and their modes of adhesion are less well established.

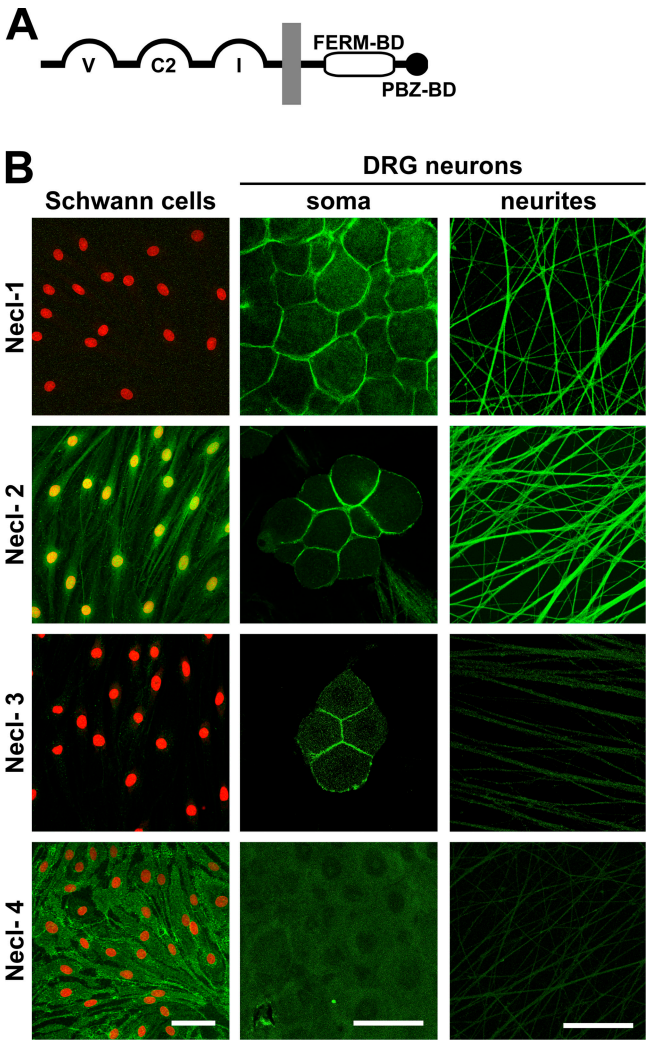

Figure 1. **Expression of Necl proteins by Schwann cells and DRG neurons.** (A) Schematic organization of the Necl protein family. The extracellular segment contains three Ig domains of the variable (V), constant-2 (C2), and intermediate (I) types; the cytoplasmic region contains FERM- and PDZ-binding motifs as indicated. (B) Staining of cultured Schwann cells (left column) and of DRG somas and neurites (middle and right columns) with antibodies to Necl-1–4 is shown. Schwann cell nuclei are stained in red. Antibodies to Necl-1, -3, and -4 recognize the ectodomain of these proteins; the Necl-2 antibody reacts with its C terminus. Necl-1 specifically stains neurons, whereas Necl-4 specifically stains Schwann cells. Necl-2 stains Schwann cell membranes, nuclei, and neurons. Necl-1–3 accumulate at sites of contact between the neuronal cell somas. Bars, 50 μm.

Because of their role in mediating cell adhesion and their linkage to 4.1 proteins, including 4.1B, which has been localized to the paranodal and juxtaparanodal domains (Ohara et al., 2000; Poliak et al., 2001; Denisenko-Nehrbass et al., 2003), we considered the Necl proteins to be candidates for the mediation of axo–glial interactions in one or more of the domains of myelinated fibers. We now report that the Necl proteins are localized to the internode of myelinated fibers in the PNS, that they bind to both axons and Schwann cells via heterophilic interactions, and that Necl-4 is up-regulated with and essential for myelination. These results implicate the Necl proteins as a major new set of cell adhesion molecules that mediate and are required for the axo–glial interactions along the internode of myelinated axons.

Results

Schwann cells and neurons express a different set of Necl proteins

To characterize their expression in axo–glial interactions and for use in functional studies, we isolated full-length cDNAs for Necl-1–4 by PCR amplification using Necl sequences present in the genomic database. An alignment of the cloned Necl protein sequences is shown in Fig. S1 A (available at http://www.jcb.org/cgi/content/full/jcb.200705132/DC1); their schematic organization is shown in Fig. 1 A.

To examine the pattern of Necl protein expression in Schwann cells, neurons, and peripheral nerves, we used a series of antibodies. These included affinity-purified polyclonal antibodies to the C termini of Necl-1 and -2; the latter were previously reported (Masuda et al., 2002; Surace et al., 2004). Analysis demonstrated that these antibodies were of high titer but exhibited some cross-reactivity with the other Necl proteins; in particular, both Necl-2 antibodies cross reacted with Necl-3 (Fig. S2 B, available at http://www.jcb.org/cgi/content/full/jcb.200705132/DC1), likely as a result of the extensive identity of the C termini of these two proteins. To generate specific antibodies to the Necl proteins, we constructed recombinant proteins containing the ectodomain of each Necl protein fused to the human Ig Fc domain. These Necl-Fc fusion proteins were individually purified and injected into guinea pigs, resulting in the generation of antisera to Necl-1, -3, and -4. Western blotting (Fig. S2 B) and immunocytochemistry of permanently transfected CHO cell lines expressing full-length Necl proteins (Fig. S2 C) corroborated the specificity of each of these antisera. For Western blot analysis, detection of the Necl proteins was markedly enhanced by treating lysates with peptide *N*-glycosidase F to remove N-linked oligosaccharides (Fig. S2 A); this likely reflects the extensive glycosylation of the Necl protein ectodomain (Masuda et al., 2002; Biederer, 2006).

We first analyzed expression of the Necl proteins by immunofluorescence of Schwann cells and dorsal root ganglion (DRG) neurons (Fig. 1 B). Necl-1 was not expressed by Schwann cells but was highly expressed at the membranes of DRG neuron cell bodies and neurites. Antibodies to the C terminus of Necl-2 stained Schwann cell membranes and nuclei and robustly stained the membranes of neurites and DRG somas. Necl-3 did not stain Schwann cells or neurites, although low level Necl-3 expression was detected at the membranes of some neuronal somas. The lack of Necl-3 expression on Schwann cells and DRG neurites suggests that their staining by Necl-2 antibodies reflects the bone fide expression of Necl-2 at these sites and is not the result of cross-reactivity with Necl-3. Necl-4 was strongly expressed at the membranes of Schwann cells, including fine filopodial-like extensions of the Schwann cell membrane (unpublished data). No staining of neurites or neuronal cell bodies by Necl-4 could be detected. These results indicate that neurons and Schwann cells express quite different sets of Necl proteins: neurites strongly express Necl-1 and -2, whereas Schwann cells principally express Necl-4 and some Necl-2. Interestingly, Necl-1–3 accumulated at sites of contact between neuronal somas in contrast to Necl-2 and -4, which were more diffusely expressed by Schwann cells.

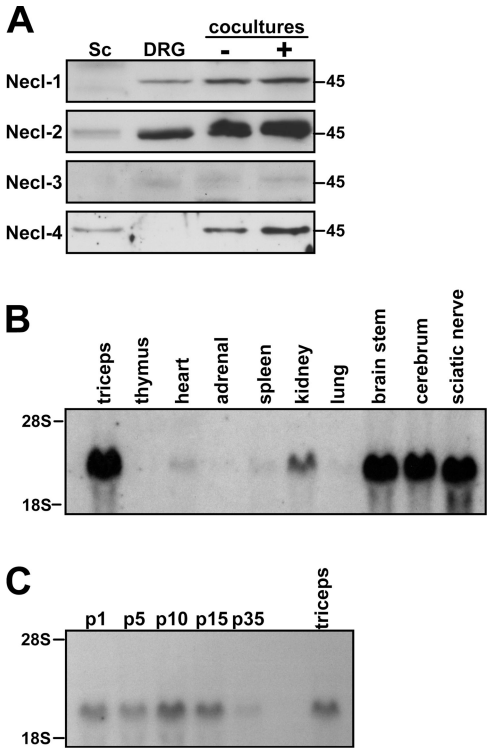

Figure 2. **Necl protein expression and Necl-4 mRNA expression.** (A) Western blot analysis of Necl protein expression by cultured Schwann cells, DRG neurons, and cocultures under nonmyelinating (−) and myelinating (+) conditions. (B) Northern blot analysis of Necl-4 mRNA expression in various tissues. (C) Northern blot analysis of Necl-4 mRNA expression at different stages of sciatic nerve development.

Western blotting of lysates after deglycosylation confirmed that Necl-1 is expressed by DRG neurons but not Schwann cells, whereas Necl-4 is expressed by Schwann cells but not by DRG neurons (Fig. 2 A). Necl-2 was expressed by Schwann cells and at substantially higher levels by DRG neurons. Each of these proteins (i.e., Necl-1, -2, and -4) accumulated in 21-d-old Schwann cell/neuron cocultures, particularly under myelinating conditions. These results strongly suggest that expression of the Necl proteins is up-regulated with myelination. We could not detect Necl-3 expression by Schwann cells and detected only faint expression in neurons by Western blotting, which is consistent with the immunofluorescence data. These latter results further indicate that the band recognized by the anti–Necl-2 antibodies in Schwann cell and neuronal lysates is indeed Necl-2.

We also examined Necl expression by PCR and Northern blot analysis. Northerns confirmed the high level expression of Necl-4 in sciatic nerves (Fig. 2 B); analysis of developing sciatic nerve demonstrated the expression of Necl- 4 mRNA perinatally that increased with myelination (Fig. 2 C). PCR analysis confirmed that Necl-1 and Necl-4 mRNA expression was principally restricted to DRG neurons and Schwann cells, respectively (Fig. S3 A, available at http://www.jcb.org/cgi/content/full/jcb.200705132/DC1), whereas Necl-2 is expressed by both cell types (Fig. S3 B). Modest differences in the expression of six previously described Necl-2

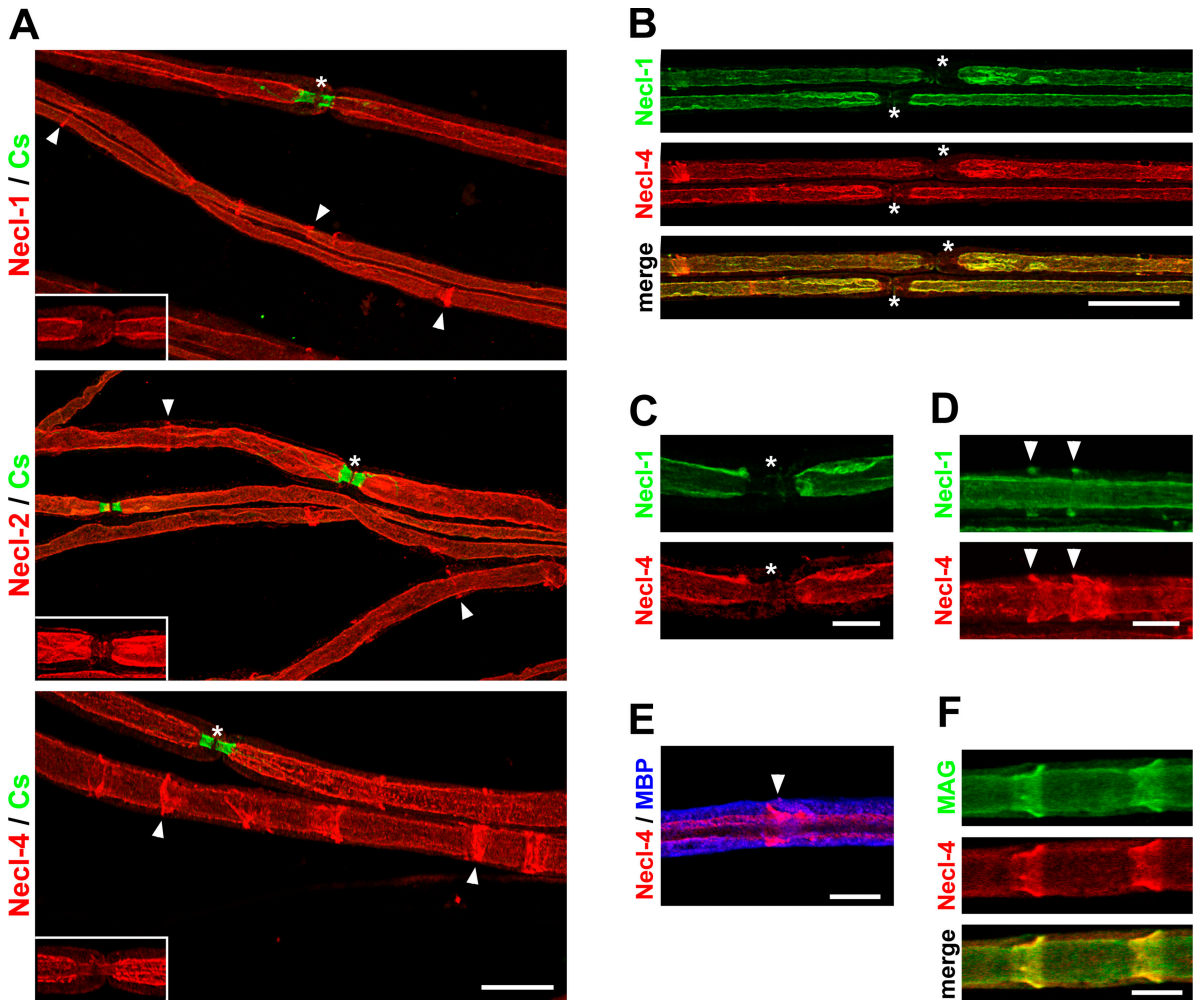

Figure 3. **The Necl proteins are localized in the internode and Schmidt-Lanterman incisures.** (A) Teased sciatic nerves from adult mice were stained with antibodies to Necl-1, -2, or -4 (red) and Caspr (green), a marker of the paranodes. Antibodies to all three Necl proteins stain the internode and Schmidt-Lanterman incisures (arrowheads). Nodes, which are indicated by asterisks, are shown magnified in the insets without Caspr staining to demonstrate that Necl expression is largely excluded from the paranodes. (B) Teased sciatic nerves were double stained for Necl-1 (green) and -4 (red); the merged image is shown below. Two nodes and their flanking paranodes located in the center of the field are indicated with asterisks and are unlabeled. (C) A node of Ranvier stained for Necl-1 (green) and -4 (red). Both Necl-1 and -4 are largely excluded from the paranodes and node, which is indicated with asterisks. (D) An internodal segment of a myelinated nerve shows two incisures (arrowheads) that are stained with antibodies to Necl-1 (green) and -4 (red). In each case, Necl-1 expression is restricted to the outer portion of these clefts, whereas Necl-4 stains the entire cleft. (E) A segment of a myelinated nerve stained for Necl-4 (red) and MBP (blue) is shown. The arrowhead indicates a Schmidt-Lanterman incisure. (F) Necl-4 (red) colocalizes with MAG (green) along the glial internode and in the clefts as shown. Bars (A and B), 25 μm; (C–F) 10 μm.

isoforms, which vary slightly in their ectodomain sequences (Biederer, 2006), were also observed by PCR analysis of neuron and Schwann cell first-strand templates (Fig. S3 B).

Necl proteins are localized at the internode of myelinated axons

To characterize the distribution of the Necl molecules in myelinated fibers, we stained adult mouse teased sciatic nerves. Staining demonstrated striking and robust expression of all three Necl proteins along the internode (i.e., the region under the compact myelin sheath extending into the juxtaparanodal region; Fig. 3 A). Necl-1 and -2 are essentially excluded from the paranodes (Fig. 3 A, insets), as indicated by the limited overlap with the paranodal marker Caspr (Einheber et al., 1997). Necl-4 is also expressed along the internode and juxtaparanodes but could be detected in some paranodes, although at reduced levels. None of the Necl proteins were detectable at the node. We were unable to detect any specific staining for Necl-3 in the teased sciatic nerves (unpublished data). These findings identify the Necl proteins as novel components of the internodal and juxtaparanodal domains.

Necl-1, -2, and -4 are also expressed at high levels in the Schmidt-Lanterman incisures of myelinating Schwann cells (Fig. 3 A, arrowheads). Necl-4 was expressed throughout all layers of the incisures, whereas Necl-1 and -2 were more variable and were frequently present only in the outermost incisural layers. The expression of Necl-1 in the incisures, a Schwann cell–specific structure, was unexpected, as Western blots demonstrated no expression of Necl-1 by Schwann cells (Fig. 2 A). Therefore, we undertook a developmental Northern analysis of Necl-1 in sciatic nerve (Fig. S3, C and D). This confirmed that Necl-1 mRNA is faintly expressed in sciatic nerve but has a

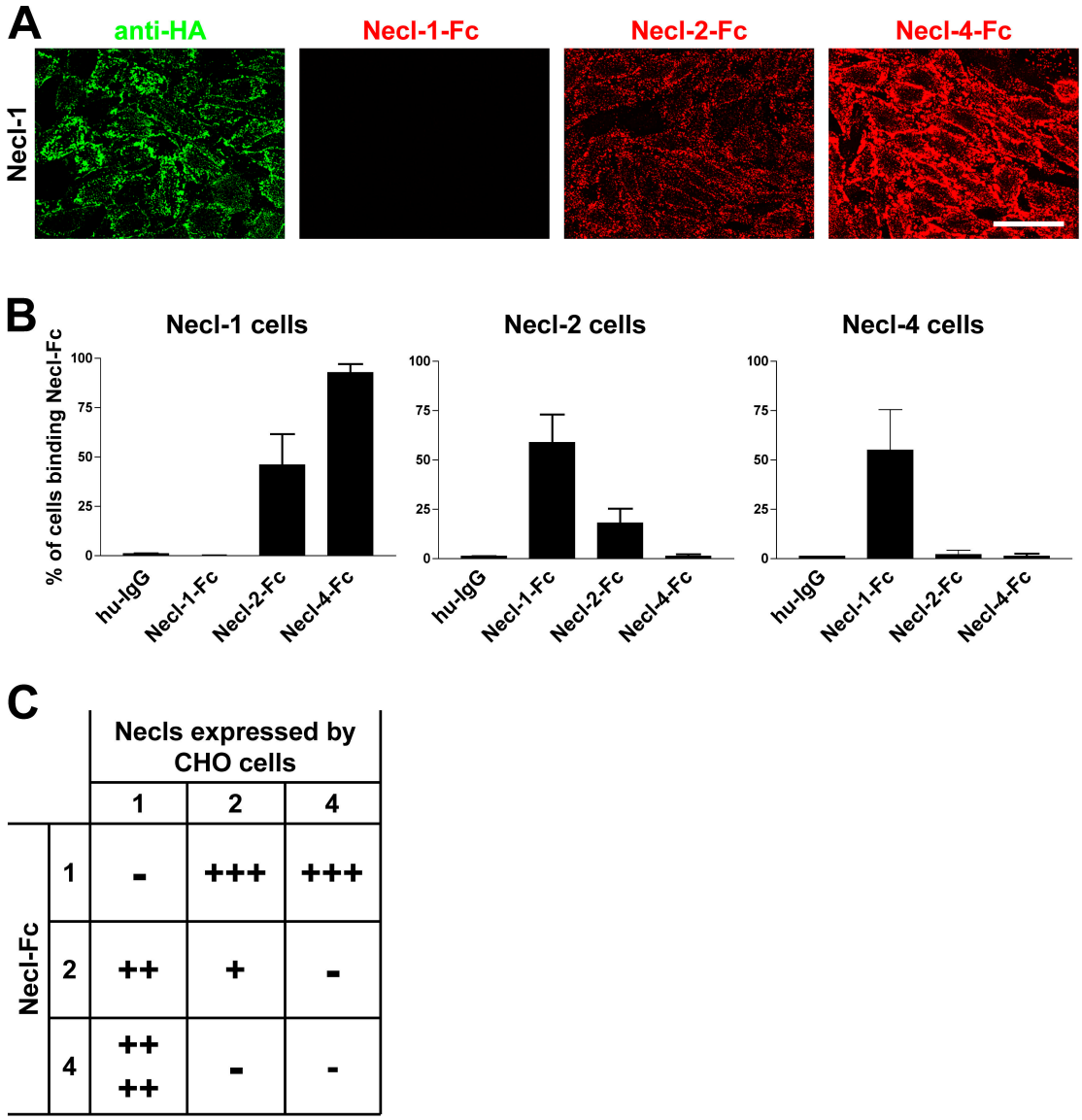

Figure 4. **Heterophilic and homophilic interactions of Necl proteins.** (A) A representative experiment demonstrating the binding of Necl-Fc constructs to monolayers of Necl-1–transfected CHO cells. Staining for the HA epitope on Necl-1 (green) and of the bound Necl proteins (red) is shown. (B) Quantitation of the results of binding of individual Necl-Fcs to each Necl-expressing CHO cell line (mean ± SEM [error bars]). The most robust binding is between Necl-1 and -4. (C) Summary of binding in the Necl family. Binding is scored as no cells (−), <25% (+), 25–50% (++), 50–75% (+++), or 75–100% (++++) of cells with bound Necl-Fc. Bar, 50 μm.

delayed onset of expression compared with Necl-4. These results demonstrate that all three of these Necl proteins are expressed in the clefts, indicating that Necl-1 and -2 expression is up-regulated in Schwann cells with myelination.

Finally, we compared the localization of Necl-1, which is enriched on axons, to Necl-4, which is expressed by Schwann cells. We stained sciatic nerves with a rabbit polyclonal antibody to the C terminus of Necl-1 and the guinea pig antibody to Necl-4. These proteins exhibited essentially identical expression patterns along the internodal domain (Fig. 3 B, yellow in the merged image). An example of a node is shown at higher magnification in Fig. 3 C. In the incisures, these proteins were frequently but not precisely colocalized; Fig. 3 D illustrates an example showing Necl-1 only in the outer layers in contrast to Necl-4, which is present throughout all layers. Double staining for myelin basic protein (MBP) confirmed that Necl-4 (Fig. 3 E, red) is localized just internal to the compact myelin sheath (Fig. 3 E, blue) adjacent to the axon. The distribution of Necl-4 in the periaxonal glial membrane and incisures is similar to that described for MAG (Trapp, 1990); double staining confirms that these proteins indeed colocalize in these domains (Fig. 3 F). Collectively, these studies indicate that Necl-1 on the axon is directly apposed by Necl-4 on the periaxonal Schwann cell membrane in the internodal domain and that the Necl proteins are new constituents of the Schmidt-Lanterman clefts.

Necl proteins preferentially mediate heterophilic interactions

To analyze their potential function in axo–glial interactions, we systematically examined the ability of the Necl proteins to

mediate homophilic or heterophilic adhesion, focusing on Necl-1, -2, and -4, which are expressed in the PNS. Interactions mediated by Necl-3, which is not expressed at detectable levels in the PNS, were also examined and are shown in Fig. S4 (available at http://www.jcb.org/cgi/content/full/jcb.200705132/DC1). To characterize binding within the Necl protein family, we incubated Necl-Fc fusion proteins with monolayers (Fig. 4 A) or dissociated cell suspensions of transfected CHO cells expressing epitope-tagged Necl proteins (Fig. S4 B). Live staining with an anti-HA antibody verified that the Necl proteins are expressed at the surface of the transfected cells (Figs. 4 A and S4) and facilitated the isolation of high level expressing cells via FACS. Necl-Fc protein binding was monitored with a fluorescently labeled anti–human Fc antibody. In the case of the dissociated CHO cells, this binding was quantitated by FACS analysis; results are summarized in Fig. 4 (B and C).

In general, the Necl proteins preferentially mediate heterophilic adhesion. The most robust binding detected was between Necl-1 and -4; substantial binding of Necl-1 to -2 was also observed as previously reported (Shingai et al., 2003). We also detected modest homophilic binding by Necl-2 but not by Necl-1 or -4. No binding of Necl-Fc proteins to control CHO cells (i.e., cells transfected with the empty pcDNA3.1 vector) was observed, indicating that Necl-Fc binding to transfected cells was specific. As axons express Necl-1 and Schwann cells principally express Necl-4, these results suggest that Necl-1 on axons binds heterophilically to Necl-4 on Schwann cells.

Necl proteins mediate adhesion to neurons and Schwann cells

We next characterized binding of the Necl proteins to purified cultures of DRG neurons and Schwann cells using a similar strategy. In general, Necl-2 and -4 bound strongly to DRG neurites, whereas Necl-1 and -2 bound robustly to Schwann cells (Fig. 5 A). No binding of Necl-1 to neurons and minimal binding of Necl-4 to Schwann cells was observed. These findings indicate that the Necl proteins mediate specific adhesion to neurons and Schwann cells.

To test the ability of the Necl proteins to promote direct Schwann cell adhesion, we examined Schwann cell attachment to Necl-Fc fusion proteins spotted onto plastic dishes at increasing concentrations; human IgG served as a control. The density of adherent Schwann cells at each Necl protein site was then measured. Representative images are shown in Fig. 5 B, and the quantitation of four separate experiments is summarized in Fig. 5 C. Schwann cells bound at high density to the substrate-adsorbed Necl-1–Fc but not to the Necl-2– or -4–Fc proteins. These results confirm that Necl-1 is able to promote Schwann cell attachment and suggest that it mediates physiologically relevant binding.

Necl-4 expression is required for Schwann cell myelination

These results highlight a potential role of the Necl proteins in general and of Necl-4 on Schwann cells in particular in the axo–glial interactions of PNS myelination. To characterize the function of the Necl proteins, we focused on Necl-4, which is the major Necl expressed by Schwann cells and is strikingly up-regulated with myelination in the cocultures (Fig. 2). For the knockdown, we targeted two distinct sequences within the first Ig domain of Necl-4 (Fig. S5 E, available at http://www.jcb.org/cgi/content/full/jcb.200705132/DC1) and subcloned the corresponding sequences into the pLL3.7 vector (Lois et al., 2002). We infected purified Schwann cells with the lentiviral short hairpin RNA (shRNA) constructs; Schwann cells infected with the empty pLL3.7 vector or pLL3.7 targeting a nonspecific sequence in luciferase (shLuc) served as controls. Both shRNAs to Necl-4 resulted in an essentially complete knockdown of Necl-4 in Schwann cells (Figs. S5 A and 6 C), whereas Necl-2 levels were unchanged, underscoring the specificity of the knockdown. Schwann cells were then added to established neuron cultures and maintained under myelinating conditions for an additional 10 d.

Knockdown of Necl-4 in Schwann cells resulted in a striking inhibition of myelin segment formation compared with control (uninfected) Schwann cells, Schwann cells infected with vector alone, or the shRNA to luciferase (Fig. 6 A). Quantitation of the number of MBP-positive myelin segments demonstrated that the shRNA constructs to Necl-4 significantly inhibited myelination, corresponding to ~75% inhibition for shNecl-4 construct #1 ($P < 0.001$) and essentially complete inhibition with the second (shNecl-4 #2) construct ($P < 0.001$). In a complementary and independent set of experiments, we also infected premyelinating neuron–Schwann cell cocultures with shRNA construct #1; myelination was then induced by the addition of ascorbate to the culture media. shRNA knockdown again resulted in the extensive inhibition of myelination in the cocultures (quantitated in Fig. S5 D). In contrast, infection of neurons with the Necl-4 shRNA construct before seeding with Schwann cells had no effect on myelination in cocultures (unpublished data).

To corroborate the specificity of the shRNA effects on myelination and to exclude nonspecific off-target effects (for review see Cullen, 2006), we performed a knockdown rescue experiment. We expressed a modified Necl-4 protein in Schwann cells treated with shRNA (construct #1); this Necl-4 protein contained codon substitutions that rendered it insensitive to shRNA treatment while preserving its amino acid sequence (Fig. S5 E). The modified Necl-4 protein was robustly expressed in shRNA-treated Schwann cells (Fig. 6 C) and, notably, fully rescued myelination (Fig. 6 A). These results underscore the specificity of the shRNA knockdown and confirm the crucial role of Necl-4 in PNS myelination. Intriguingly, overexpression of the Necl-4 construct may enhance myelination in the cocultures based on increased numbers of myelin segments (Fig. 6 B). These results suggest that Necl-4 may provide a positive signal for myelination.

Schwann cells remained associated with axons despite the knockdown of Necl-4 based on phase microscopy (unpublished data) and immunofluorescence staining (Fig. S5 F). Schwann cell numbers were comparable in the knockdown cultures (Hoechst stain; Fig. 6 A). Western blot analysis of the effects of Necl-4 knockdown corroborated the inhibition of myelin protein expression (Fig. 6 C) and also demonstrated substantial effects on Schwann cell transcription factor expression (Fig. 6 D). Thus, there was dramatic inhibition of Oct-6, a

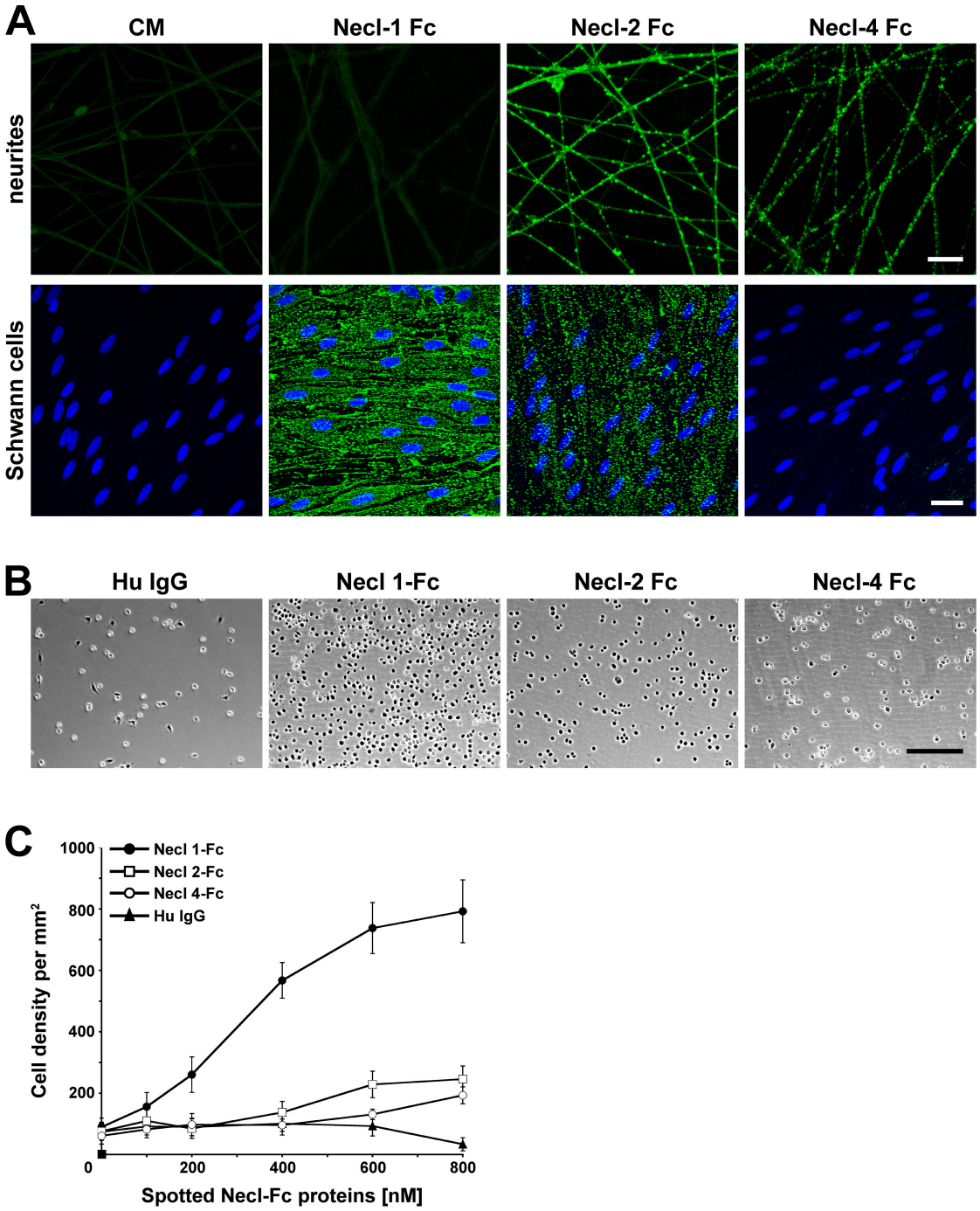

Figure 5. **Binding of Necl proteins to DRG neurons and Schwann cells.** (A) Conditioned media from nontransfected cells (CM) or cells transfected with individual Necl-Fc constructs were incubated with cultures of DRG neurons (top) or Schwann cells (bottom). Bound Fc constructs were visualized with fluorescein-ated anti–human IgG. Necl-1 Fc binds to Schwann cells but not neurons; Necl-4-Fc binds to neurons but not Schwann cells. (B) Representative phase images of Schwann cell binding to Necl-Fc proteins. Dissociated Schwann cells were incubated with plastic substrates spotted with human IgG (control) or purified Necl-Fc constructs. (C) Quantitation of the binding of Schwann cells to Necl-Fc constructs spotted onto dishes at the different concentrations indicated (mean ± SEM [error bars]). Schwann cells bound robustly only to the Necl-1–Fc substrate. Bars (A), 25 μm; (B) 200 μm.

transcription factor expressed by promyelinating Schwann cells (Scherer et al., 1994), and nearly complete inhibition of the expression of Krox-20, a transcription factor required for the myelinating phenotype of Schwann cells (Topilko et al., 1994). These results indicate that Necl-4 expression is required for progression to the promyelinating stage and subsequent myelination of axons.

Necl-1 on axons mediates binding to Necl-4 on Schwann cells

Finally, we tested the effects of knockdowns of Necl-1 and -4 on the binding of Necl proteins to axons and Schwann cells. Knockdown of Necl-4 effectively ablated the expression of Necl-4 at the Schwann cell membrane (Fig. 7 A, a). In the absence of Necl-4, Necl-1 no longer bound to Schwann cells (Fig. 7 A, c).

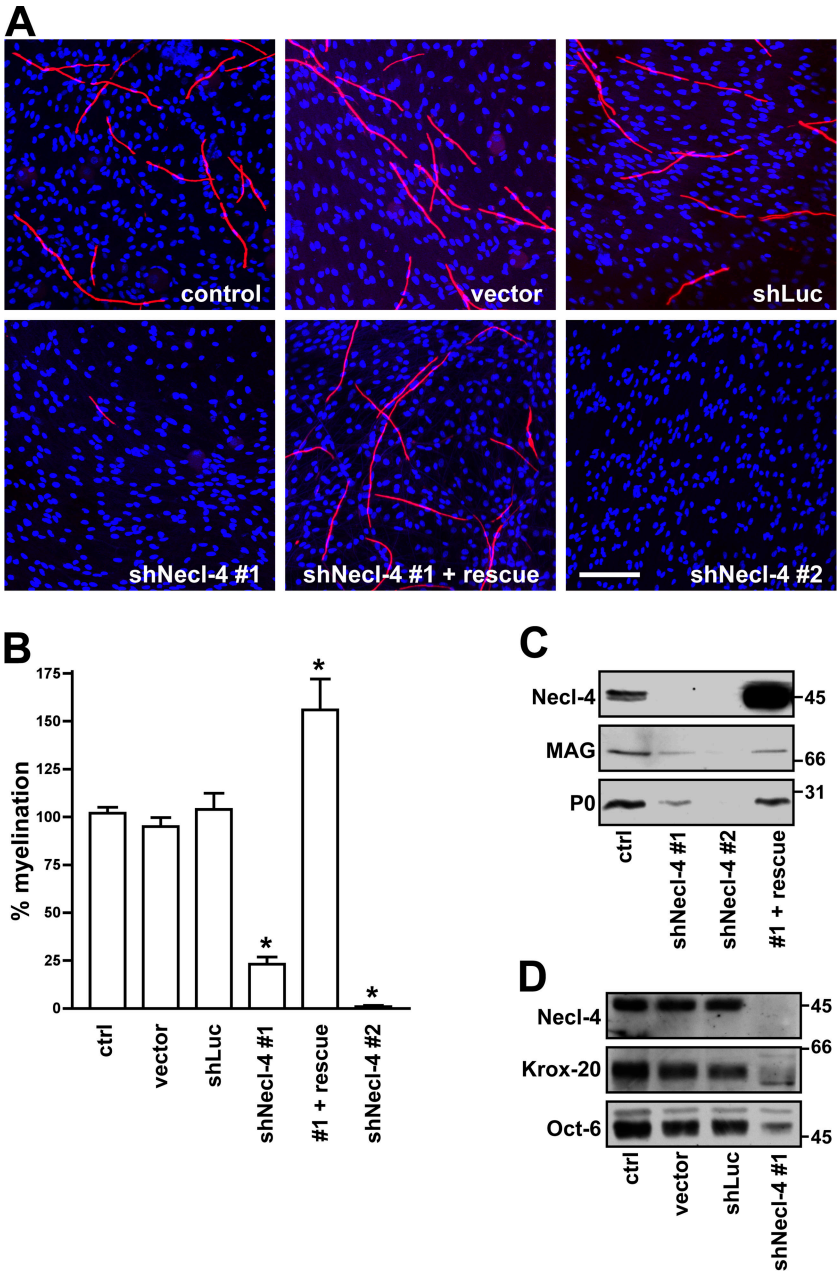

Figure 6. **Necl-4 expression is required for Schwann cell differentiation and myelination.** (A) Representative images of myelinating cocultures in which control Schwann cells or Schwann cells infected with the lentiviral vector alone or lentiviruses encoding shRNA to a nonspecific sequence (shLuc) or to Necl-4 sequences, in one case rescued with an exogenous Necl-4 protein (shNecl-4 #1 + rescue), were added to DRG neurons under myelinating conditions. Myelin segments were stained for MBP (red) and with the Hoechst nuclear dye (blue). (B) Quantitation of the effects of Necl-4 knockdowns on Schwann cell myelination. Control Schwann cells or Schwann cells infected with the lentiviral vector alone or viruses encoding shRNAs to luciferase or Necl-4 with or without rescue by an shRNA-resistant Necl-4 were seeded onto dissociated DRG neuron cultures and maintained under myelinating conditions for 10 d. The number of myelin segments that formed were quantitated from three separate experiments (mean ± SEM [error bars]); controls were normalized to 100%. *, $P < 0.001$. (C) Knockdown of Necl-4 inhibits myelin protein expression. Lysates from control Schwann cells and cells infected with lentiviruses encoding shRNAs to Necl-4, including cells rescued with a modified Necl-4 protein, were blotted for Necl-4 and the myelin proteins MAG and P0; cultures correspond to those shown in Fig. 6 A. shRNA treatment effectively knocked down Necl-4 and myelin protein and was restored by the overexpression of an shRNA-resistant Necl-4. (D) Knockdown of Necl-4 inhibits the expression of myelin transcription factors. Western blot analysis demonstrates the substantial knockdown of Necl-4 and corresponding reductions of the transcription factors Krox-20 and Oct-6. Bar, 100 μm.

In contrast, Necl-2 still bound to Schwann cells in the absence of Necl-4 (Fig. 7 A, e), indicating that its binding is independent of Necl-4. In complementary studies, we performed a knockdown of Necl-1 on neurons by lentiviral-mediated shRNA (Fig. 7 B). This effectively inhibited Necl-1 expression based on Western blotting (Fig. S5 B). In the absence of Necl-1, Necl-4 binding to neurites was substantially reduced (Fig. 7 B). Together, these results indicate that Necl-1 on the axon and Necl-4 on the Schwann cell are obligate binding partners.

Discussion

We have demonstrated that neurons and Schwann cells express distinct members of the Necl protein family. We also show that the Necl proteins preferentially mediate heterophilic interactions (with Necl-1 on the axon binding to Necl-4 on the Schwann cell), that these proteins delineate the internodal domain, and that Necl-4 mediates axonal–glial interactions required for myelination. These results have important implications for the domain organization of axons and the mechanisms that initiate Schwann cell myelination, as considered further below.

Schwann cells and DRG neurons express distinct sets of Necl proteins

Previous studies demonstrated that the Necl proteins are expressed in the nervous system. Necl-1 expression was found to be largely restricted to the developing and adult nervous system (Fig. S3, C and D; Fukami et al., 2003; Zhou et al., 2005). Necl-2 and -4 are also highly expressed in the nervous system (Biederer et al., 2002; Fukami et al., 2002; Fujita et al., 2005)

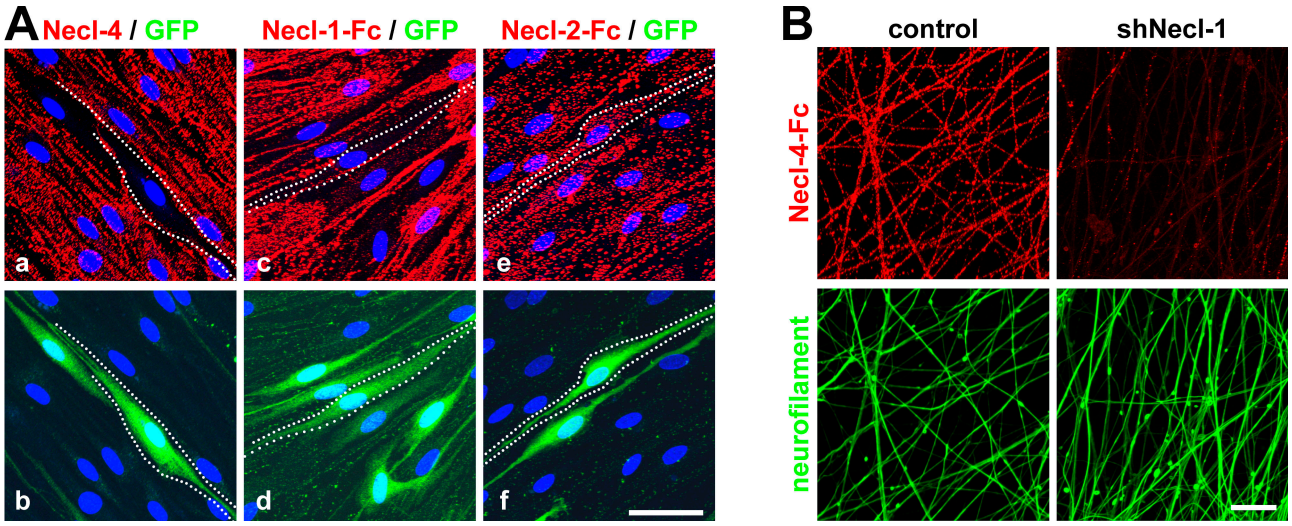

Figure 7. **Necl-4 on Schwann cells binds to Necl-1 on axons.** (A) Schwann cells were infected with a dilution of the lentivirus encoding shRNA (construct #1) to Necl-4. Effects of shRNA treatment on Necl-4 expression (a) and the binding of Necl-1–Fc (c) and Necl-2–Fc (e); corresponding fields shown below (b, d, and f) are stained for GFP to identify infected cells. Examples of infected cells are outlined by dashed white lines. (B) Necl-4–Fc does not bind to axons in the absence of Necl-1. shRNA-treated neurons were incubated with Necl-4–Fc; robust binding is seen in control but not shRNA-treated neurites. The corresponding Western blot is shown in Fig. S5 C (available at http://www.jcb.org/cgi/content/full/jcb.200705132/DC1). Bottom panels show the same fields stained for neurofilament. Bars (A), 25 μM; (B) 40 μm.

but are more broadly distributed: Necl-2 is expressed by a variety of epithelial tissues, and Necl-4 is highly expressed by the kidney, bladder, and prostate (Fig. 2 B; Fukuhara et al., 2001; Williams et al., 2006). The primary sites of Necl-3 expression still remain to be elucidated.

Our results extend these studies and indicate that neurons and Schwann cells express different sets of Necl proteins. Thus, DRG neurons preferentially express Necl-1 and -2, whereas Schwann cells preferentially express Necl-4 and, at lower levels, Necl-2 (Figs. 1 and 2). PCR data also indicate that neurons and Schwann cells preferentially express Necl-1 and Necl-4, respectively (Fig. S3 A). We were unable to detect the expression of Necl-3 on axons, Schwann cells, or sciatic nerve by blotting or immunostaining, indicating that Necl-3 is unlikely to contribute to axon–Schwann cell interactions. Low levels of Necl-3 were present at sites of contact between neuronal cell bodies.

Heterophilic interactions between Necl-1 and -4 mediate axon–Schwann cell interactions

We systematically characterized all potential interactions within the Necl family (Figs. 4 and S4), substantially extending previous analyses. Our data demonstrate that the Necl proteins preferentially mediate heterophilic rather than homophilic interactions. The strongest interactors among the three Necl proteins expressed in the PNS are Necl-1 with Necl-4. Necl-1 also strongly binds to Necl-2, consistent with the accumulation of both of these proteins at sites of neuronal contact (Fig. 1 B). Homophilic interactions of Necl-2 were detected (Fig. 4) as previously reported (Biederer et al., 2002; Masuda et al., 2002) but were less robust. We were unable to detect homophilic adhesion mediated by Necl-1 or by Necl-4; the former result contrasts with recent studies (Kakunaga et al., 2005; Dong et al., 2006). Thus, Necl-1 and -4 likely function physiologically as heterophilic adhesion molecules.

An interaction of axonal Necl-1 with Schwann cell Necl-4 is strongly supported by several lines of evidence. Necl-1 and -2 are localized along the internodal axon in a pattern that is essentially identical to that of Necl-4 on the apposed Schwann cell membrane (Fig. 3 B). However, although axons express both Necl-1 and -2, Schwann cells only attached to substrates patterned by the Necl-1–Fc protein (Fig. 5). Knockdown of Necl-4 abolished Necl-1 but not Necl-2 binding to Schwann cells; similarly, knockdown of Necl-1 abolished the binding of Necl-4 to axons (Fig. 7). These latter results confirm that Necl-1 on axons binds specifically to Necl-4 on Schwann cells and suggest that the low level expression of Necl-2 on Schwann cells does not contribute appreciably to Necl-1 adhesion.

As noted, Necl-2 is also expressed at high levels along the internode (Fig. 3 A). Although both neurons and Schwann cells are potential sources of Necl-2 along the internode, immunostaining of cultured cells suggests that this expression is largely neuronal (Fig. 1 B). Preliminary immuno-EM with a Necl-2 antibody further suggests that neurons are an important source of Necl-2 expression in the internode but also confirms the high level expression of Necl-2 in the Schmidt-Lanterman incisures (unpublished data). As Necl-2 binds to Schwann cells in a Necl-4–independent manner, its ligand on the Schwann cells remains to be determined. Necl-2 may bind via weak homophilic interactions to Schwann cells, where it is also expressed at reduced levels (Figs. 1 B and 2 A). However, clustering of the Necl-2–Fc bound to Schwann cells recruits only limited amounts of endogenous Necl-2 (not depicted), and Necl-2 does not accumulate at sites of contact between Schwann cells (Fig. 1 B). Thus, Necl-2 may bind to Schwann cells by a Necl-independent mechanism. Necl-2 has several known heterophilic ligands,

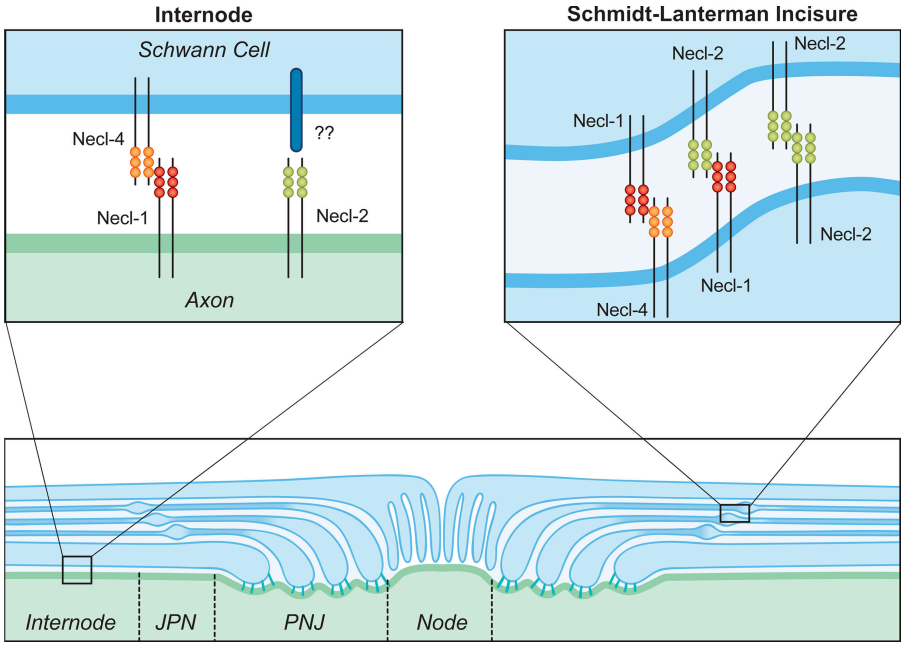

Figure 8. **Summary of Necl protein interactions within domains of myelinated fibers.** Schematic diagram showing the domain organization of a myelinated axon and the potential interactions between the Necl proteins in the internode and Schmidt-Lanterman incisures. In the internode and juxtaparanodes (JPN), Necl-1 on the axon binds to Necl-4 on the Schwann cell. Necl-2 is also present on the axon; its interacting partners on the Schwann cell are not yet known. The Necl proteins are also heavily expressed in the Schmidt-Lanterman incisures of mature myelinated nerves; Necl-1 and -2 are expressed primarily in the outer portions of the clefts (indicated), whereas Necl-4 is expressed in all layers. Potential interactions in the clefts of Necl-1 with Necl-4 and -2 and homophilic interactions of Necl-2 are illustrated. There is essentially no expression of the Necl proteins in the paranodal junctions (PNJ) or at the node. Necl proteins are shown as cis-dimers predicted from structural data.

including Nectin-3 (Shingai et al., 2003) and the class I major histocompatibility complex–restricted T cell–associated molecule, an Ig cell adhesion molecule expressed on activated T cells (Arase et al., 2005; Boles et al., 2005). Whether either of these ligands is expressed by Schwann cells and mediates binding to Necl-2 on axons will require additional investigation. Collectively, our results suggest that Necl-1 and Necl-2 on the axon bind to Schwann cells via Necl-4 and via an as yet unknown Schwann cell receptor, respectively. The expression and putative trans-interactions of Necl proteins in the internode are summarized in Fig. 8.

Necl protein complexes delineate the internodal domain and Schmidt-Lanterman incisures

With the identification of the Necl proteins as mediators of axon–glial interactions in the internode, key adhesion complexes in each of the domains of myelinated axons have now been identified. Thus, like other domains of myelinated axons (Poliak and Peles, 2003; Salzer, 2003; Schafer and Rasband, 2006), the internode contains a specific set of glial cell adhesion molecules that bind to cognate adhesion molecules on the axon. In addition to their expression in the internode, the Necl proteins are also present in the juxtaparanodes, where they are likely to supplement the axo–glial interactions mediated by TAG-1 and Caspr2 (Poliak et al., 2003; Traka et al., 2003). The Necl proteins are largely excluded from the paranodes (Fig. 3), although Necl-4 expression does extend into some glial paranodes at modest levels.

The Schmidt-Lanterman clefts are the other major site of Necl expression in mature myelinated nerves (Fig. 3 A). Necl-1 and -2 are highly expressed together with Necl-4 in this Schwann cell–specific site; their localization at this site, together with epithelial cadherin (E-cadherin; Fannon et al., 1995) and MAG (Fig. 3 F), presumably contributes to organization of the incisures. Binding preferences suggest interactions of Necl-1 with -4 and Necl-1 with -2 at this site (Fig. 8). The precise nature of the interactions remains to be established, as Necl-1 and -4 do not consistently colocalize in all layers of the clefts (Fig. 3 D). Accumulation of the Necl proteins in the clefts may also contribute to the increased expression that occurs during myelination, as detected by Western blotting of the cocultures (Fig. 2 A). The presence of Necl-1 in the clefts also indicates that it is not strictly neuron specific but rather that it is upregulated in Schwann cells with myelination; the latter finding was confirmed by Northern blots of developing sciatic nerve (Fig. S3 D).

The presence of the Necl proteins along the internode and in the clefts further suggests several candidate proteins with which they may interact at these sites. The Necl proteins contain a conserved FERM-binding domain in their cytoplasmic sequence and have been reported to interact biochemically with the members of the 4.1 protein family, including Necl-1 with 4.1N (Zhou et al., 2005) and Necl-2/TSLC1 with a truncated form of 4.1B (Yageta et al., 2002). In agreement, we have identified 4.1 proteins along the internode and in the clefts (unpublished data). The Necl proteins also contain a class II PDZ domain–binding motif at their C terminus that mediates their interactions with membrane-associated guanylate kinase family members. Necl-1 and -2 can interact with PDZ domain proteins CASK (Biederer et al., 2002; Kakunaga et al., 2005), PASL2 (Shingai et al., 2003), and Dlg3 (Kakunaga et al., 2005). A variety of membrane-associated guanylate kinase proteins are known to be concentrated in the incisures (Poliak et al., 2002) and, therefore, are candidates to interact with the C terminus of the Necl proteins. Finally, we note that MAG is coexpressed with Necl-4 at high levels in the glial periaxonal membrane in the internode and in the clefts. Whether MAG interacts either in cis (i.e., with Necl-4) or in trans (i.e., with Necl-1 or -2) is not yet known.

Necl-4 is essential for myelination

A key finding of this study is that Necl-4 has an essential role in the initial axo–glial interactions required for myelination. Knockdown of Necl-4 (Figs. 6 and S5) efficiently blocks Schwann cell differentiation and myelination, as indicated by the absence of myelin proteins and myelin segments. The limited expression of Oct-6 and Krox-20 in the knockdown cocultures indicates that Schwann cells are arrested before progressing to the promyelinating stage. Thus, Necl-4 is critical for axonal signaling that drives Schwann cell differentiation and myelination.

A key question is how Necl-4 mediates these effects. One possibility is that in the absence of Necl-4, axon–Schwann cell apposition and interactions are impaired, preventing effective signaling from the axon. A major axonal signal for myelination is type III neuregulin 1, which is required for Schwann cell differentiation and regulates myelin sheath thickness (Michailov et al., 2004; Taveggia et al., 2005). Initial results demonstrate that Necl-4–deficient Schwann cells still attach to and amplify in association with axons (Fig. S5 F), which is in contrast to the aberrant interactions Schwann cells display with neuregulin-deficient axons (Taveggia et al., 2005). Although preliminary, these results suggest that other adhesion molecules can promote the attachment of Schwann cells to the axon (Wanner and Wood, 2002) and that Necl-4 may have a distinct role in promoting Schwann cell differentiation and myelination. Of potential interest, the Necl proteins have been implicated in promoting cell polarity (for review see Ogita and Takai, 2006), which is a critical early event required for the initiation of Schwann cell myelination (Chan et al., 2006; Taveggia and Salzer, 2007). Whether Necl-4 interacts with components of the polarity complex implicated in myelination (Chan et al., 2006), as suggested by its localization at the inner glial turn and its PDZ-binding sequences, will be of interest for future study.

In summary, these findings suggest that Necl-4 has several key roles in axo–glial interactions: a crucial role in promoting Schwann cell differentiation and myelination, a potentially related role in organizing the internodal domain by binding to Necl-1 on the axon, and an additional role with Necl-1 and -2 in organizing the Schmidt-Lanterman incisures. Elucidating the events downstream of Necl-4 signaling and its potential role in central nervous system myelination are likely to provide important additional insights into the axo–glial signaling of myelination.

Materials and methods

Isolation of cDNAs for Necl proteins

Total RNA was isolated from purified rat Schwann cells or rat DRG neurons with the RNAqueous-4PCR kit (Ambion); mRNA from mouse brain was purified using the mRNA isolation kit (Roche). First-strand templates were prepared by RT-PCR with an oligo-dT primer (Promega). cDNAs for Necl-1–4 were amplified using primers based on rodent sequences and cloned into the pcDNA3.1 directional TOPO cloning vector (Invitrogen).

To clone the rat Necl-1, sense (ATGGGGGCCCCTTCCGCCCT) and antisense (CTAGATGAAATATTCCTTCTTGTCATCCCCGCC) primers were used to PCR amplify a full-length cDNA from rat DRG neuron first strand (GenBank/EMBL/DDBJ accession no. DQ272743). To clone Necl-2, we designed primers based on the mouse cDNA for TSLC1 (Fukami et al., 2002). We amplified a full-length cDNA from adult mouse brain with sense (ATGGCGAGTGCTGTGCTGCC) and antisense (CTAGAAGTACTCTTTCTTTTCTTCGGAGTT) primers. This mouse isoform of Necl-2 corresponds to isoform 4 of SynCAM 1 (Biederer et al., 2002) that lacks the putative mucin-like domain of the predicted rat sequence. The mouse Necl-2 cDNA is available from GenBank/EMBL/DDBJ (accession no. DQ279856). Necl-3 was amplified from rat Schwann cell first strand using sense (ATGATTTGGAAACGCAG) and antisense (TTAAATGAAATACTCTTTTTTCTC) primers, and the sequence is available from GenBank/EMBL/DDBJ (accession no. DQ272744). A full-length Necl-4 cDNA was amplified from rat Schwann cell first strand using sense (ATGGGCCGGGCCCGGCGCTTCC) and antisense (AATGAAGAATTCTTCTTTCCGTTTGTGTCCATCGCCGC) primers, and the sequence is available from GenBank/EMBL/DDBJ (accession no. DQ272745).

Generation of permanently transfected CHO cell lines expressing Necl proteins

CHO cells were transfected with full-length constructs for each Necl protein and with the empty pcDNA3.1 vector using the LipofectAMINE 2000 reagent (Invitrogen); permanently transfected cells were selected by maintenance in G418-containing medium (α-MEM, 10% FBS, and 750 μg/ml G418). To facilitate analysis, the sequence encoding the influenza HA epitope was added by PCR to the N terminus of each Necl protein immediately after the signal peptide as predicted by the SignalP program. CHO cells were stained for the HA epitope and selected by FACS (MoFlo; DakoCytomation).

Generation of Necl-Fc fusion proteins

Constructs encoding the extracellular domain of each Necl protein fused to the hinge region of the human IgG-Fc were subcloned into the pcDNA 3.1 TOPO vector (Invitrogen) and transiently transfected into HEK 293FT cells (Invitrogen). Transfected cells were maintained in media containing DME, 1% Ultra Low IgG FBS (Invitrogen), 1 mM nonessential amino acids (Invitrogen), and 2 mM L-glutamine. Conditioned media was collected after 3 d and alkalinized by 1 M Hepes buffer (Invitrogen) at 10% vol, and the salt concentration was increased by adding 10× Dulbecco's PBS (dPBS) at 25% vol. The conditioned media was then filtered, and Necl-Fc proteins were collected batchwise with protein A–agarose beads (Roche). The beads were washed with 6× dPBS plus 0.2% Triton X-100 (Sigma-Aldrich) followed by 6× dPBS and 1× dPBS washes. The proteins were eluted off the beads with 200 mM glycine buffer at pH 2.8, immediately neutralized with 1 M Hepes, pH 8.5, at 10% vol, and dialyzed overnight against dPBS (1:500 vol/vol) using Slide-A-Lyser dialysis cassettes (Pierce Chemical Co.). Protein concentrations were assessed with the BCA Protein Assay (Pierce Chemical Co.). Biochemical analysis confirmed that each construct encoded proteins of the predicted size of ∼65 kD after deglycosylation.

Antibodies and immunofluorescence

Guinea pig polyclonal antibodies were generated against Necl-1, -3, and -4 by immunization with the corresponding Necl-Fc fusion protein. Antibodies to the human Fc moiety were removed by passing antiserum over an agarose–human IgG (Jackson ImmunoResearch Laboratories) column. Rabbit polyclonal antibodies to Necl-2 have previously been described (Masuda et al., 2002; Surace et al., 2004). A rabbit polyclonal antibody was raised to the C-terminal sequence (AEGGQSGGDDKKEYFI) of Necl-1 coupled to keyhole limpet hemocyanin and injected into rabbits, and the resulting antibodies were affinity purified against the immunizing peptide coupled to Sepharose beads. Other antibodies included mouse monoclonal antibodies to MBP (SMI-94) and neurofilament (SMI-31 and SMI-32; all obtained from Sternberger Monoclonals) and the HA epitope (HA.11; Covance). Polyclonal antibodies specific to Krox-20 and Oct-6 (provided by D. Meijer, Erasmus University, Rotterdam, Netherlands), Caspr (gifts from E. Peles [Weizmann Institute, Rehovot, Israel] and M. Bhat [University of North Carolina, Chapel Hill, NC]), MAG (Pedraza et al., 1990), and neurofilament (Covance) were also used. Secondary antibodies included donkey anti–mouse (FITC, rhodamine X, Cy5, and amino-methylcoumarin conjugated), donkey anti–guinea pig (FITC and rhodamine X conjugated), donkey anti–rabbit (FITC and rhodamine X conjugated), donkey anti–chicken (Cy5 and amino-methylcoumarin conjugated), and goat anti–human-Fc (FITC and rhodamine X conjugated; Jackson ImmunoResearch Laboratories). For FACS analysis, we also used phycoerythrin (PE)-conjugated donkey anti–mouse (eBioscience).

Immunofluorescent preparations were examined by epifluorescence on a confocal microscope (LSM 510; Carl Zeiss MicroImaging, Inc.). Confocal images were acquired with Neofluor 40× NA 1.3 oil or Apochromat 63× NA 1.4 oil objectives (Carl Zeiss MicroImaging, Inc.) on an 8-bit photomultiplier tube (Carl Zeiss MicroImaging, Inc.) using LSM software (Carl Zeiss MicroImaging, Inc.). In some cases, brightness and contrast were adjusted with Photoshop 7.0 (Adobe).

Neuron and Schwann cell cultures

Establishment of primary rat Schwann cell and DRG neuron cultures has been described previously (Einheber et al., 1993). In brief, neurons were isolated from embryonic day 16 DRGs by trypsinization and plated on a collagen substrate (Biomedical Technologies Inc.) in standard neuronal medium (neurobasal medium, 2% B27 supplement, 2 mM L-glutamine, 0.4% glucose, and 50 ng/ml 2.5S NGF). Nonneuronal cells were removed by feeding the cultures every 2 d alternately with standard neuronal medium supplemented or not supplemented with 5-fluorodeoxyuridine and uridine (both at 10 μM) over a week. Schwann cells prepared from postnatal day 2 sciatic nerves (Brockes et al., 1979) were expanded in D media (DME, 10% FBS, and 2 mM L-glutamine) supplemented with 4 μM forskolin and 5 ng/ml of the EGF domain of rhNRG-1-β1 (over a period of 2–3 wk; R&D Systems). Schwann cells were then maintained in D media for 3 d before use. Myelinating Schwann cell–neuron cocultures were established by seeding purified DRG neuron cultures with 200,000 Schwann cells in C media (MEM, 10% FBS, 2 mM L-glutamine, 0.4% glucose, and 50 ng/ml 2.5S NGF). After 3 d, cocultures were supplemented with 50 μg/ml ascorbic acid to initiate basal lamina formation and myelination and were maintained for an additional 10–21 d.

DME was obtained from BioWhittaker Bioproducts. α-MEM, MEM, neurobasal media, B27 supplement, L-glutamine, trypsin, and G418 were purchased from Life Technologies. Glucose, forskolin, 5-fluorodeoxyuridine, uridine, and ascorbic acid were purchased from Sigma-Aldrich. FBS was obtained from Gemini, and NGF was purchased from Harlan Bioproducts.

Preparation of teased sciatic nerves

Sciatic nerves were removed from 10–12-mo-old C57BL mice, fixed with 4% PFA (Electron Microscopy Sciences) for 2 h, and stored in dPBS (Invitrogen) at 4°C until teased. Teased sciatic nerve fibers were mounted on glass slides, dried overnight at room temperature, and stored at −80°C until use for immunofluorescence staining.

Necl binding and FACS analysis

To analyze the binding of Necl proteins to Schwann cells, DRG neurons, and CHO-Necl clones, cells were rinsed with L15 medium (Invitrogen) and incubated for 45 min at RT with conditioned media from transiently transfected HEK 293FT cells secreting specific Necl-Fcs. Cultures were washed once with L15 and incubated with a FITC- or rhodamine X–conjugated goat anti–human Fc for 45 min at room temperature. After washing with dPBS, cultures were fixed with 4% PFA. Schwann cells and CHO-Necl clones were mounted in the presence of Hoechst dye (Invitrogen) nuclear stain. DRG neurons were further stained for neurofilaments before mounting.

To further characterize homophilic versus heterophilic Necl binding, we performed a FACS analysis with Necl-Fc constructs. CHO cells expressing Necl proteins were briefly trypsinized for 1 min with 0.125% trypsin and 0.5 mM EDTA at room temperature, collected in ice-cold HBSS medium (Invitrogen) containing 10% FBS to terminate trypsinization, and washed twice in HBSS medium. Cells were diluted in HBSS to a final concentration of 750,000 cells in 200 μl and incubated with either one of the Necl-Fc proteins or whole human IgG at a final concentration of 200 nM; cells were incubated on ice for 30 min. Anti-HA antibody at 1:500 was also added to detect the CHO-Necl cells. After incubation, cells were washed once with ice-cold HBSS and incubated with PE-conjugated donkey anti–mouse (to detect expressing cells) and FITC-conjugated anti–human Fc (to detect Necl-Fc binding; both at 1:100) for 30 min on ice. After two washes in ice-cold HBSS and one wash in Ca^{2+}/$Mg2^{+}$-free ice-cold dPBS, fluorescence measurements of individual cells were performed using FACS (FACScan; Becton Dickinson). Log fluorescence was collected for FITC (channel FL1-H) and PE (channel FL2-H) and displayed as double-parameter (PE/FITC) graphs. For each CHO-Necl clone, the FL2-H channel was calibrated by labeling cells for the HA tag only (no FITC), whereas the FITC channel (no PE) was calibrated by detecting Necl-Fc, giving the strongest binding as determined initially by binding to cells in culture. Additional controls included omitting anti-HA antibodies and Necl-Fc proteins, with only PE- and FITC-conjugated secondary antibodies added. Analysis was first gated on single cells on the basis of forward and side light scatter based on data acquisition from 10,000 cells. Each CHO-Necl clone was incubated with human IgG as a control. The FITC fluorescence value below which 99% of the events were found was noted and used as the boundary between no binding versus binding (Fig. S4 B, left and right red boxes). Binding of Necl-Fc was determined by counting the number of cells in the binding gate and dividing by the total number of cells. FACS analysis was performed with the FlowJo software package (Tree Star, Inc.).

Cell adhesion assay

Necl-Fc proteins serially diluted in HBSS were spotted (2 μl/spot) onto 100-mm nontissue culture polystyrene dishes (Fisherbrand; Fisher Scientific) to minimize nonspecific cell attachment to the plastic. Duplicate spots were made for each dilution of Necl-Fc per experiment. Plates were incubated in a 37°C tissue culture incubator for 1 h, washed twice with HBSS, blocked with 1% BSA in HBSS for 1 h at 37°C, washed twice with HBSS, and washed once with D media. Schwann cells were briefly trypsinized, resuspended in D media at a density of 250,000 cells/ml, and 10 ml were added to each plate. The cultures were incubated in a 10% CO_2 and 37°C tissue culture incubator for 90 min. The plates were then gently washed with dPBS twice, and cells were fixed with 4% PFA. Phase-contrast digital images of the spots (10× fields) were captured with a microscope (Eclipse TE2000-U; Nikon), and the number of cells per field was determined using ImageJ software (National Institutes of Health).

RNAi of Necl proteins

To generate shRNAs, we used the pLentiLox (pLL3.7) vector in which the U6 promoter drives shRNA expression and GFP is expressed under separate promoter control (provided by L. Van Parijs; Rubinson et al., 2003; Dillon et al., 2005). Two 21 nucleotide shRNAs (#1: nt 79–99, GTGCAGACAGAGAATGTGACG; #2: nt 151–171, GGGTCTATAGTCGTCATTCAG) that targeted sequences within the first IgG domain of Necl-4 were designed using Easy siRNA (ProteinLounge), BLOCK-iT RNAi designer (Invitrogen), and siRNA sequence selector (CLONTECH Laboratories, Inc.). The shRNA stem loops for pLL3.7 vector were designed to contain a sense shRNA sequence followed by a short (9 nt) nonspecific loop sequence and an antisense shRNA sequence followed by six thymidines, which serve as a stop signal for RNA polymerase III. The 5′-phosphorylated PAGE-purified oligonucleotides were annealed and subcloned into HpaI–XhoI sites of pLL3.7. The lentiviral vector was transfected into 293FT cells together with packaging plasmids Δ8.9 and pCMV-VSVG (provided by J. Milbrandt, Washington University, St. Louis, MO) using LipofectAMINE 2000 (Invitrogen). As controls, we used the empty pLL3.7 vector or a vector encoding shRNA to a nonspecific (luciferase) sequence. Viral supernatants were collected 72 h after transfection, centrifuged at 3,000 rpm for 15 min, aliquoted for one-time use, and frozen at −80°C. An shRNA targeting a 21-nt sequence (nt 733–753; GTGCAGACAGAGAATGTGACG) in the third IgG domain of Necl-1 was designed using the same approach.

For rescue experiments, a codon-modified Necl-4 construct was generated using the QuikChange XL Site-Directed Mutagenesis kit (Stratagene). The sequence GTGCAGACAGAGAATGTGACG (nt 79–99) was replaced with sequence GTACAAACGGAAAACGTAACA, which did not change the amino acid composition of Necl-4 but rendered the construct insensitive to the Necl-4–specific shRNA #1. The modified Necl-4 was subcloned into the pLenti6/V5 Directional Topo vector (Invitrogen), and viral production was performed as per the pLL3.7 constructs.

Freshly plated Schwann cells (10^6 cells per 100-mm plate) were incubated for 3 d with viruses at a 2/3 dilution (vol/vol) in D media (DME, 10% FBS, and 2 mM L-glutamine) supplemented with forskolin and rhNRG-β1 (EGF domain). Cells were expanded for an additional week and maintained for 3 d in D media before use. Protein knockdowns were confirmed by Western blotting and by immunohistochemistry.

Northern blot analysis

RNA was isolated from rat sciatic nerves and Schwann cells by $CsCl_2$ gradient centrifugation (Chirgwin et al., 1979). Equal amounts (10 μg) of total RNA were electrophoresed in 1% agarose and 2.2 M formaldehyde gels, transferred to nylon membranes (Duralon; Stratagene) in 6× SSC, and UV cross-linked (0.12 J). Blots were prehybridized, hybridized, and washed using standard techniques; the final stringency of the wash was 0.2× SSC at 65°C for 30 min (Sambrook et al., 1989). cDNAs corresponding to nt 1–981 of rat Necl-1 and nt 1–966 of rat Necl-4 were used as probes. The probes were generated by PCR, isolated by agarose gel electrophoresis, and purified with the QIAquick Gel Extraction kit (QIAGEN). ^{32}P-labeled cDNA probes with specific activities of 2–5 × 10^9 cpm/μg were prepared by primer extension with random hexamers using the Prim-a-gene kit (Promega) according to the manufacturer's instructions

Software

Sequence alignments were performed with the Clustal V program (Higgins, 1994). The Necl proteins were analyzed for the presence of putative domains using the following programs and databases: SignalP (Nielsen et al., 1997) and TMHHM (Nielsen and Krogh, 1998), Pfam (Bateman et al., 2004), SMART (Schultz et al., 1998), and Scansite 2.0 (Obenauer

et al., 2003). Statistical analysis was performed with the Prism software package (GraphPad).

Online supplemental material

Fig. S1 presents amino acid sequences of the Necl proteins. Fig. S2 shows Necl expression CHO cell lines and specificity of anti-Necl antibodies. Fig. S3 shows PCR of Necl-2 isoforms and Northern analysis of Necl-1. Fig. S4 presents the binding of Necl-Fc fusion proteins to Necl-expressing cells. Fig. S5 shows that the knockdown of Necl-4 inhibits myelination in cocultures. Online supplemental material is available at http://www.jcb.org/cgi/content/full/jcb.200705132/DC1.

We thank Carla Taveggia for helpful discussions, Jill Gregory for assistance with illustrations, Jeff Milbrandt for lentiviral packaging plasmids, and Dies Meijer, Manzoor Bhat, and Ori Peles for providing antibodies.

This study was supported by a National Institutes of Health grant (NS43474 to J.L. Salzer), a National Multiple Sclerosis Society grant (RG 3439-A-9 to J.L. Salzer), and a Department of Defense grant (DAMD-17-04-0266 to D.H. Gutmann).

Submitted: 21 May 2007
Accepted: 27 July 2007

References

Arase, N., A. Takeuchi, M. Unno, S. Hirano, T. Yokosuka, H. Arase, and T. Saito. 2005. Heterotypic interaction of CRTAM with Necl2 induces cell adhesion on activated NK cells and CD8+ T cells. *Int. Immunol.* 17:1227–1237.

Bateman, A., L. Coin, R. Durbin, R.D. Finn, V. Hollich, S. Griffiths-Jones, A. Khanna, M. Marshall, S. Moxon, E.L. Sonnhammer, et al. 2004. The Pfam protein families database. *Nucleic Acids Res.* 32:D138–D141.

Biederer, T. 2006. Bioinformatic characterization of the SynCAM family of immunoglobulin-like domain-containing adhesion molecules. *Genomics*. 87:139–150.

Biederer, T., Y. Sara, M. Mozhayeva, D. Atasoy, X. Liu, E.T. Kavalali, and T.C. Sudhof. 2002. SynCAM, a synaptic adhesion molecule that drives synapse assembly. *Science*. 297:1525–1531.

Boles, K.S., W. Barchet, T. Diacovo, M. Cella, and M. Colonna. 2005. The tumor suppressor TSLC1/NECL-2 triggers NK-cell and CD8+ T-cell responses through the cell-surface receptor CRTAM. *Blood*. 106:779–786.

Brockes, J.P., K.L. Fields, and M.C. Raff. 1979. Studies on cultured rat Schwann cells. I. Establishment of purified populations from cultures of peripheral nerve. *Brain Res.* 165:105–118.

Chan, J.R., C. Jolicoeur, J. Yamauchi, J. Elliott, J.P. Fawcett, B.K. Ng, and M. Cayouette. 2006. The polarity protein Par-3 directly interacts with p75NTR to regulate myelination. *Science*. 314:832–836.

Chirgwin, J.M., A.E. Przbyla, R.J. MacDonald, and R.J. Rutter. 1979. Isolation of biologically active ribonucleic acid from sources enriched in ribonuclease. *Biochemistry*. 18:5294–5299.

Cullen, B.R. 2006. Enhancing and confirming the specificity of RNAi experiments. *Nat. Methods*. 3:677–681.

Denisenko-Nehrbass, N., K. Oguievetskaia, L. Goutebroze, T. Galvez, H. Yamakawa, O. Ohara, M. Carnaud, and J.A. Girault. 2003. Protein 4.1B associates with both Caspr/paranodin and Caspr2 at paranodes and juxtaparanodes of myelinated fibres. *Eur. J. Neurosci.* 17:411–416.

Dillon, C.P., P. Sandy, A. Nencioni, S. Kissler, D.A. Rubinson, and L. Van Parijs. 2005. RNAi as an experimental and therapeutic tool to study and regulate physiological and disease processes. *Annu. Rev. Physiol.* 67:147–173.

Dong, X., F. Xu, Y. Gong, J. Gao, P. Lin, T. Chen, Y. Peng, B. Qiang, J. Yuan, X. Peng, and Z. Rao. 2006. Crystal structure of the V domain of human Nectin-like molecule-1/Syncam3/Tsll1/Igsf4b, a neural tissue-specific immunoglobulin-like cell-cell adhesion molecule. *J. Biol. Chem.* 281:10610–10617.

Einheber, S., T.A. Milner, F. Giancotti, and J.L. Salzer. 1993. Axonal regulation of Schwann cell integrin expression suggests a role for $\alpha 6\ \beta 4$ in myelination. *J. Cell Biol.* 123:1223–1236.

Einheber, S., G. Zanazzi, W. Ching, S. Scherer, T.A. Milner, E. Peles, and J.L. Salzer. 1997. The axonal membrane protein Caspr, a homologue of neurexin IV, is a component of the septate-like paranodal junctions that assemble during myelination. *J. Cell Biol.* 139:1495–1506.

Fannon, A.M., D.L. Sherman, G. Ilyina-Gragerova, P.J. Brophy, V.L. Friedrich Jr., and D.R. Colman. 1995. Novel E-cadherin-mediated adhesion in peripheral nerve: Schwann cell architecture is stabilized by autotypic adherens junctions. *J. Cell Biol.* 129:189–202.

Fujita, E., K. Urase, A. Soyama, Y. Kouroku, and T. Momoi. 2005. Distribution of RA175/TSLC1/SynCAM, a member of the immunoglobulin superfamily, in the developing nervous system. *Brain Res. Dev. Brain Res.* 154:199–209.

Fukami, T., H. Satoh, E. Fujita, T. Maruyama, H. Fukuhara, M. Kuramochi, S. Takamoto, T. Momoi, and Y. Murakami. 2002. Identification of the Tslc1 gene, a mouse orthologue of the human tumor suppressor TSLC1 gene. *Gene*. 295:7–12.

Fukami, T., H. Satoh, Y.N. Williams, M. Masuda, H. Fukuhara, T. Maruyama, M. Yageta, M. Kuramochi, S. Takamoto, and Y. Murakami. 2003. Isolation of the mouse Tsll1 and Tsll2 genes, orthologues of the human TSLC1-like genes 1 and 2 (TSLL1 and TSLL2). *Gene*. 323:11–18.

Fukuhara, H., M. Kuramochi, T. Nobukuni, T. Fukami, M. Saino, T. Maruyama, S. Nomura, T. Sekiya, and Y. Murakami. 2001. Isolation of the TSLL1 and TSLL2 genes, members of the tumor suppressor TSLC1 gene family encoding transmembrane proteins. *Oncogene*. 20:5401–5407.

Gomyo, H., Y. Arai, A. Tanigami, Y. Murakami, M. Hattori, F. Hosoda, K. Arai, Y. Aikawa, H. Tsuda, S. Hirohashi, et al. 1999. A 2-Mb sequence-ready contig map and a novel immunoglobulin superfamily gene IGSF4 in the LOH region of chromosome 11q23.2. *Genomics*. 62:139–146.

Gruber-Olipitz, M., J.W. Yang, I. Slavc, and G. Lubec. 2006. Nectin-like molecule 1 is a high abundance protein in cerebellar neurons. *Amino Acids*. 30:409–415.

Hannila, S.S., M.M. Siddiq, and M.T. Filbin. 2007. Therapeutic approaches to promoting axonal regeneration in the adult mammalian spinal cord. *Int. Rev. Neurobiol.* 77:57–105.

Higgins, D.G. 1994. CLUSTAL V: multiple alignment of DNA and protein sequences. *Methods Mol. Biol.* 25:307–318.

Hirano, A. 1983. Reaction of the periaxonal space to some pathologic processes. *In* Progress in Neuropathology. vol. 5. H.M. Zimmerman, editor. Raven Press, New York. 99–112.

Ikeda, W., S. Kakunaga, K. Takekuni, T. Shingai, K. Satoh, K. Morimoto, M. Takeuchi, T. Imai, and Y. Takai. 2004. Nectin-like molecule-5/Tage4 enhances cell migration in an integrin-dependent, Nectin-3-independent manner. *J. Biol. Chem.* 279:18015–18025.

Ito, A., T. Jippo, T. Wakayama, E. Morii, Y. Koma, H. Onda, H. Nojima, S. Iseki, and Y. Kitamura. 2003. SgIGSF: a new mast-cell adhesion molecule used for attachment to fibroblasts and transcriptionally regulated by MITF. *Blood*. 101:2601–2608.

Kakunaga, S., W. Ikeda, S. Itoh, M. Deguchi-Tawarada, T. Ohtsuka, A. Mizoguchi, and Y. Takai. 2005. Nectin-like molecule-1/TSLL1/SynCAM3: a neural tissue-specific immunoglobulin-like cell-cell adhesion molecule localizing at non-junctional contact sites of presynaptic nerve terminals, axons and glia cell processes. *J. Cell Sci.* 118:1267–1277.

Kuramochi, M., H. Fukuhara, T. Nobukuni, T. Kanbe, T. Maruyama, H.P. Ghosh, M. Pletcher, M. Isomura, M. Onizuka, T. Kitamura, et al. 2001. TSLC1 is a tumor-suppressor gene in human non-small-cell lung cancer. *Nat. Genet.* 27:427–430.

Li, C., M.B. Tropak, R. Gerlai, S. Clapoff, W. Abramow-Newerly, B. Trapp, A. Peterson, and J. Roder. 1994. Myelination in the absence of myelin-associated glycoprotein. *Nature*. 369:747–750.

Lois, C., E.J. Hong, S. Pease, E.J. Brown, and D. Baltimore. 2002. Germline transmission and tissue-specific expression of transgenes delivered by lentiviral vectors. *Science*. 295:868–872.

Martini, R., and M. Schachner. 1986. Immunoelectron microscopic localization of neural cell adhesion molecules (L1, N-CAM, and MAG) and their shared carbohydrate epitope and myelin basic protein in developing sciatic nerve. *J. Cell Biol.* 103:2439–2448.

Masuda, M., M. Yageta, H. Fukuhara, M. Kuramochi, T. Maruyama, A. Nomoto, and Y. Murakami. 2002. The tumor suppressor protein TSLC1 is involved in cell-cell adhesion. *J. Biol. Chem.* 277:31014–31019.

Michailov, G.V., M.W. Sereda, B.G. Brinkmann, T.M. Fischer, B. Haug, C. Birchmeier, L. Role, C. Lai, M.H. Schwab, and K.A. Nave. 2004. Axonal neuregulin-1 regulates myelin sheath thickness. *Science*. 304:700–703.

Montag, D., K.P. Giese, U. Bartsch, R. Martini, Y. Lang, H. Blüthmann, J. Karthigasan, D.A. Kirschner, E.S. Wintergerst, K.-A. Nave, et al. 1994. Mice deficient for the myelin-associated glycoprotein show subtle abnormalities in myelin. *Neuron*. 13:229–246.

Murakami, Y. 2005. Involvement of a cell adhesion molecule, TSLC1/IGSF4, in human oncogenesis. *Cancer Sci.* 96:543–552.

Nielsen, H., and A. Krogh. 1998. Prediction of signal peptides and signal anchors by a hidden Markov model. *Proc. Int. Conf. Intell. Syst. Mol. Biol.* 6:122–130.

Nielsen, H., J. Engelbrecht, S. Brunak, and G. von Heijne. 1997. Identification of prokaryotic and eukaryotic signal peptides and prediction of their cleavage sites. *Protein Eng.* 10:1–6.

Obenauer, J.C., L.C. Cantley, and M.B. Yaffe. 2003. Scansite 2.0: Proteome-wide prediction of cell signaling interactions using short sequence motifs. *Nucleic Acids Res.* 31:3635–3641.

Ogita, H., and Y. Takai. 2006. Nectins and nectin-like molecules: roles in cell adhesion, polarization, movement, and proliferation. *IUBMB Life*. 58:334–343.

Ohara, R., H. Yamakawa, M. Nakayama, and O. Ohara. 2000. Type II brain 4.1 (4.1B/KIAA0987), a member of the protein 4.1 family, is localized to neuronal paranodes. *Brain Res. Mol. Brain Res.* 85:41–52.

Pedraza, L., G.C. Owens, L.A.D. Green, and J.L. Salzer. 1990. The myelin-associated glycoproteins: membrane disposition, evidence of a novel disulfide linkage between immunoglobulin-like domains, and post-translational palmitylation. *J. Cell Biol.* 111:2651–2661.

Poliak, S., and E. Peles. 2003. The local differentiation of myelinated axons at nodes of Ranvier. *Nat. Rev. Neurosci.* 4:968–980.

Poliak, S., L. Gollan, D. Salomon, E.O. Berglund, R. Ohara, B. Ranscht, and E. Peles. 2001. Localization of Caspr2 in myelinated nerves depends on axon-glia interactions and the generation of barriers along the axon. *J. Neurosci.* 21:7568–7575.

Poliak, S., S. Matlis, C. Ullmer, S.S. Scherer, and E. Peles. 2002. Distinct claudins and associated PDZ proteins form different autotypic tight junctions in myelinating Schwann cells. *J. Cell Biol.* 159:361–372.

Poliak, S., D. Salomon, H. Elhanany, H. Sabanay, B. Kiernan, L. Pevny, C.L. Stewart, X. Xu, S.Y. Chiu, P. Shrager, A.J. Furley, and E. Peles. 2003. Juxtaparanodal clustering of Shaker-like K+ channels in myelinated axons depends on Caspr2 and TAG-1. *J. Cell Biol*. 162:1149–1160.

Rubinson, D.A., C.P. Dillon, A.V. Kwiatkowski, C. Sievers, L. Yang, J. Kopinja, D.L. Rooney, M.M. Ihrig, M.T. McManus, F.B. Gertler, et al. 2003. A lentivirus-based system to functionally silence genes in primary mammalian cells, stem cells and transgenic mice by RNA interference. *Nat. Genet.* 33:401–406.

Sakisaka, T., and Y. Takai. 2004. Biology and pathology of nectins and nectin-like molecules. *Curr. Opin. Cell Biol.* 16:513–521.

Salzer, J.L. 2003. Polarized domains of myelinated axons. *Neuron*. 40:297–318.

Sambrook, J., E.F. Fritsch, and T. Maniatis. 1989. Molecular Cloning: a Laboratory Manual. Cold Spring Harbor Laboratory, Cold Spring Harbor, NY. 1659 pp.

Schafer, D.P., and M.N. Rasband. 2006. Glial regulation of the axonal membrane at nodes of Ranvier. *Curr. Opin. Neurobiol.* 16:508–514.

Scherer, S.S., D.Y. Wang, R. Kuhn, G. Lemke, L. Wrabetz, and J. Kamholz. 1994. Axons regulate Schwann cell expression of the POU transcription factor SCIP. *J. Neurosci.* 14:1930–1942.

Schultz, J., F. Milpetz, P. Bork, and C.P. Ponting. 1998. SMART, a simple modular architecture research tool: identification of signaling domains. *Proc. Natl. Acad. Sci. USA*. 95:5857–5864.

Shingai, T., W. Ikeda, S. Kakunaga, K. Morimoto, K. Takekuni, S. Itoh, K. Satoh, M. Takeuchi, T. Imai, M. Monden, and Y. Takai. 2003. Implications of nectin-like molecule-2/IGSF4/RA175/SgIGSF/TSLC1/SynCAM1 in cell-cell adhesion and transmembrane protein localization in epithelial cells. *J. Biol. Chem.* 278:35421–35427.

Surace, E.I., E. Lusis, Y. Murakami, B.W. Scheithauer, A. Perry, and D.H. Gutmann. 2004. Loss of tumor suppressor in lung cancer-1 (TSLC1) expression in meningioma correlates with increased malignancy grade and reduced patient survival. *J. Neuropathol. Exp. Neurol.* 63:1015–1027.

Taveggia, C., and J.L. Salzer. 2007. PARsing the events of myelination. *Nat. Neurosci.* 10:17–18.

Taveggia, C., G. Zanazzi, A. Petrylak, H. Yano, J. Rosenbluth, S. Einheber, X. Xu, R.M. Esper, J.A. Loeb, P. Shrager, et al. 2005. Neuregulin-1 type III determines the ensheathment fate of axons. *Neuron*. 47:681–694.

Topilko, P., S. Schneider-Maunoury, G. Levi, A. Baron-Van Evercooren, A.B. Chennoufi, T. Seitanidou, C. Babinet, and P. Charnay. 1994. Krox-20 controls myelination in the peripheral nervous system. *Nature*. 371:796–799.

Traka, M., L. Goutebroze, N. Denisenko, A. Nifli, S. Havaki, Y. Iwakura, F. Fukamauchi, K. Watanabe, B. Soliven, J.A. Girault, and D. Karagogeos. 2003. Association of TAG-1 with Caspr2 is essential for the molecular organization of juxtaparanodal regions of myelinated fibers. *J. Cell Biol.* 162:1161–1172.

Trapp, B.D. 1990. The myelin-associated glycoprotein: location and potential functions. *In* Myelination and Dysmyelination. vol. 605. D. Colman, I. Duncan, and R. Skoff, editors. The New York Academy of Sciences, New York. 29–43.

Urase, K., A. Soyama, E. Fujita, and T. Momoi. 2001. Expression of RA175 mRNA, a new member of the immunoglobulin superfamily, in developing mouse brain. *Neuroreport*. 12:3217–3221.

Wanner, I.B., and P.M. Wood. 2002. N-cadherin mediates axon-aligned process growth and cell-cell interaction in rat Schwann cells. *J. Neurosci.* 22:4066–4079.

Williams, Y.N., M. Masuda, M. Sakurai-Yageta, T. Maruyama, M. Shibuya, and Y. Murakami. 2006. Cell adhesion and prostate tumor-suppressor activity of TSLL2/IGSF4C, an immunoglobulin superfamily molecule homologous to TSLC1/IGSF4. *Oncogene*. 25:1446–1453.

Yageta, M., M. Kuramochi, M. Masuda, T. Fukami, H. Fukuhara, T. Maruyama, M. Shibuya, and Y. Murakami. 2002. Direct association of TSLC1 and DAL-1, two distinct tumor suppressor proteins in lung cancer. *Cancer Res.* 62:5129–5133.

Yu, R.C., and R.P. Bunge. 1975. Damage and repair of the peripheral myelin sheath and node of Ranvier after treatment with trypsin. *J. Cell Biol.* 64:1–14.

Zhou, Y., G. Du, X. Hu, S. Yu, Y. Liu, Y. Xu, X. Huang, J. Liu, B. Yin, M. Fan, et al. 2005. Nectin-like molecule 1 is a protein 4.1N associated protein and recruits protein 4.1N from cytoplasm to the plasma membrane. *Biochim. Biophys. Acta*. 1669:142–154.